

Performance of Variable Electrical Field (VEF) on Casson Flow Through an Inclined Annular Micro-Channel Embedded in a Porous Medium: Numerical Solution by Using Spectral Collocation Method

Adebowale Martins Obalalu*

Department of Statistics and Mathematical Sciences, Kwara State University, Malete, Nigeria

Received March 17, 2021; Accepted August 9, 2021

Abstract

This study aims to examine the impact of Variable Electrical Field (VEF) on blood rheological (Casson) fluid flow through a micro annular channel embedded in a porous medium. The implication of is to generate electromagnetohydrodynamic force function the Variable electrical field (VEF) has been considered as a function of temperature. In most of the literature, the thermophysical properties of the fluid are assumed to be unchanged. However, this present study bridges this gap by assuming that viscosity, conductivity, and electrical field are all temperature-dependent. The current study provides fast convergent methods on the finite interval, namely Spectral collocation method (SCM) are used to analyzes the fluid flow, temperature field, skin friction, and Nusselt number. The equations controlled were first non-dimensional and then simplified by a similarity transformation to ordinary nonlinear differential equations. It was deduced that; the flow field was reduced as variable thermal and electrical field parameters were increased. This finding has a significant impact on the treatment of hyperthermia, especially in terms of understanding/regulating blood flow.

Keywords Variable electrical field (VEF); Blood rheological (Casson); Electromagnetohydrodynamic; Spectral collocation method (SCM).

1. Introduction

In modern scientific and engineering problems, Magnetohydrodynamics (MHD) is one of the important areas for progress. Moreover, this scientific area can also be regarded as a subsection of fluid mechanics dealing with reciprocal interactions between a magnetic field externally applied and electrically leading fluid flows [1]. These various applications will occur with the MHD flow phenomenon in the MHD flux of biomagnetic fluids like human blood, with fluid dynamics and heat transfer problems [2]. In different fields of bioengineering and medical science that use blood as the moving biological fluid, this issue is very useful. Besides, blood is well known to have a magnetically moving function and an important role to play in transportation through the human body of substrates and other molecules between tissues and organs [3]. The work of Hartmann and Lazarus first conducted an experimental trial of the new MHD stream in a lab [4]. Initially, Hartmann and Lazarus carried out experiments with modern MHD flow in a laboratory. Also, a theoretical analysis of mixed convection and MHD effect was discussed by [5]. The work of Oja and Giresha use a numerical method to analyze the hall effects on a couple of stress fluid with heat generation impact [6].

The ability of a material to conduct heat is measured by its thermal conductivity. It is well known that when a fluid is exposed to heat, its physical properties can change dramatically. The heat generated by inner friction and the corresponding increase in temperature in lubricating fluids affects of viscosity cannot be underestimated. Temperature increase gives rise to a local increase in the phenomena of transport, by reducing viscosity across the momentum boundary layer, which also greatly influences the wall heat transfer rate. Fluids can undergo extreme conditions in industrial systems, such as high temperature and pressure, high shear rates, and external heating (environmental heating), each of which can result in high fluid

temperatures. Each substance defining its thermal conductivity is distinguished by its peculiarity. It plays an important role in the transfer of heat. Due to its extensive examples in industry and engineering, there has been a concern about temperature conductivity. Several scholars [7-9] assumed physical properties like thermal conductivity to be constant, however, practical results show that thermal conductivity is strongly influenced by temperature differences, particularly when they are large. The influence of viscosity is deliberated as constant in numerous soundings. The work of Rahman *et al.* studied the effect of variable viscosity and thermal conductivity effects in the micropolar flux movement [10]. Their research shows that the thermal conductivity and slip increase the thickness of the energy limit layer. The mixed convection with variable viscosity and convection of water in the boundary layer over a non-stationary vertical plate is studied by [11]. It was shown that the free-stream speed has a significant impact on the speed profile.

A microchannel is a semiconductor cylinder that enhances electrical flow. In fluid controlling and heat transfer, microchannels are used [12]. The geometry of micro-fluidic systems is extremely important, consequently, the import of convective transport phenomena in microchannels and micronutrients has dramatically increased in [13]. Scientists have provided research on heat transfer and pressure drop for laminar flow in microchannels in recent years [14]. Obalalu [3] exhibited that the utilizing of rheological CF to enhance the behavior of thermodynamics for better cooling. Hari and Harshad [15] discussed the Importance of Radiative Casson fluid and the chemical reaction of Hydromagnetic flow passing through an oscillating vertical plate. A semi-analytical study has been performed by Obalalu [1] in examining the rheological Casson fluid on hydrodynamic Natural Convective flow with a porous material. Other recent geometrical investigations of porous annuli include buoyant convection production in double-passage vertical annuli with unheated entry and porosity [16]. Sankar *et al.* investigated magneto-convective heat transfer in vertical porous annuli using a computational model to examine the viscous dissipation [17]. The production of natural convection in vertical porous annuli subjected to isothermal adiabatic thermal conditions and the electro magnetohydrodynamic flow with the irreversible study of a porous asymmetric microchannel under the influence of Joule heating was proposed by [18]. Obalalu *et al.* [19] scrutinized the magnetic field and heat generation effect on unsteady vertical hydrodynamic flow through a porous channel with convective boundary conditions.

In many branches of many fields of science, engineering, and food processing, Casson fluid (CF) has received significant attention. Oil, honey, jelly, and paint are common examples of common commodities exhibiting CF properties [1]. Casson fluid (CF) is a non-Newtonian fluid with shear thinning, yield stress, and high shear viscosity. It acts like an elastic solid at low shear strain, while it acts like a Newtonian fluid at above critical yield stress [20]. Casson first established the CF model [21]. The study defines the pigment-oil suspension prediction flow. The Newtonian fluid model was shown to decrease to non-Newtonian fluid particularly when the stress on the wall is above the yield stress. CF flow from hydromagnetic and thermal convection heat transfer to a stretched permeable surface was reported [22].

There has been no consideration of the impact of variable electronic conductivity in the above study. Engineers can take sufficient electrical conductivity from fluids to regulate several metallurgical processes. The use of fourth order Runge-Kutta method and shooting iteration scheme has been used to investigate steady MHD convection flow, with variable electrical conductivity and thermal generation along with an isothermal vertical plate [23]. Chen, and Dani [24] investigated Impact of Maxwell-Wagner polarization on soil complex dielectric permittivity in the existence of electrical conductivity. They assumed that electrical conductivity varies with temperature and that the Prandtl number is low.

As a follow-up to the aim, the comprehensive discussion of the current scientific manuscript requires adequate answers to some motivating research questions. Here are a few examples, but not exclusively:

1. What is the relevant way to express variable electrical conductivity, thermal conductivity, and variable viscosity on blood rheological (Casson) fluid flow?

2. How can the Skin friction along with the Nusselt number benefit from using Annular Micro-Channel?
3. what is the effect of the thermophysical properties, Casson parameter, heat source parameter, melting parameter, Hartman number, suction/injection parameter on blood rheological (Casson) fluid flow through the micro annular channel in the existence of variable electrical conductivity?
4. How can the blood rheological (Casson) be apply Numerically using the spectral collocation method (SCM)?

This present work will provide adequate answers to this scientific questions. This study believes the assumption of constant fluid properties looks unrealistic, however this present study bridges this gap by assuming that viscosity, conductivity, and electrical field are all temperature-dependent.

2. Model formulation

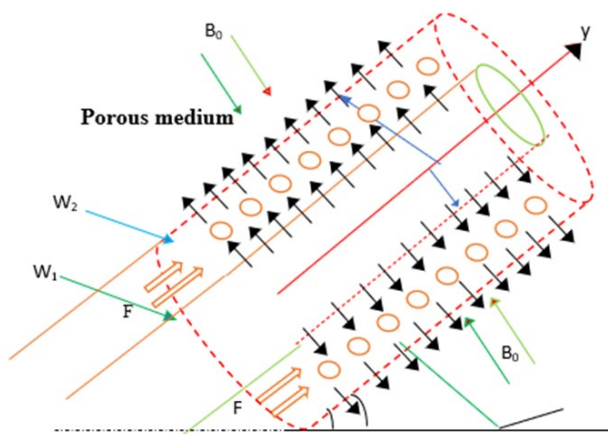


Figure 1. Physical model coordinate system

The thermophysical/electrical properties of blood rheological fluid motion in an inclined micro annular porous channel with slip/jump effect were assumed variable in the flow assumption of steady, MHD conducting, fully developed, incompressible, and dissipative fluid flow transfer of heat and nonlinear convective process of heat transfer. The annular walls are subjected differently to heat with the outer surface of the inner porous cylinder sustained at a temperature W_1 while the inner surface of the outer porous cylinder at a temperature W_2 . Natural convection takes place because of the diversity of temperatures. Figure 1 showing the outer

and inner cylinder radii of the microchannel suspended at an angle π , C_1 and C_0 while the y axis is moved into the flow path, the x axis is moved into the microchannel.

$$\nabla \cdot \vec{F} = 0 \tag{1}$$

$$\rho([\vec{F} \cdot \nabla]\vec{F}) = J \times B_0 + \mu \nabla^2 \vec{F} - \frac{\mu}{k_p} \vec{F} - \rho_K g \cos[\alpha] - \nabla P \tag{2}$$

$$\rho c_p([\vec{F} \cdot \nabla]T) = \kappa \nabla^2 T + \mu(\nabla \vec{F} \cdot \nabla \vec{F}) + Q \tag{3}$$

The kinematic viscosity, variable viscosity, and thermal conductivity as an exponential function of temperature, a variable electrical conductivity as a linear temperature function, and the buoyancy force non-linear representation are as follows for an isentropic and incompressible Casson fluid.

$$\begin{aligned} \mu(T) &= \mu_0 e^{-\gamma_1(W-W_0)}, \quad \kappa(T) = \kappa_0 e^{-\gamma_2(W-W_0)}, \quad \sigma^* = \sigma_0[1 + \gamma_0(W - W_0)], \quad \rho_K \\ &= -[k_a(W - W_0) + k_b(W - W_0)^2], \quad \nu = \left(1 + \frac{1}{C}\right) \frac{\mu}{\rho} \end{aligned} \tag{4}$$

To estimate the suction/injection rate at the cylinder surfaces, we assume the suction/injection at the outer surface of the inner cylinder to be as $F = F_0$ while injection/suction rate at the inner surface of the outer cylinder is taken to be $F = F_0 \frac{d_1}{d_0}$. Integrating Equation (1) we obtain

$$F = F_0 \frac{d_1}{d} \tag{5}$$

The following are the governing systems for electrically conducting, fully developed, Casson fluid flow through an inclined porous medium the assumptions of fluid properties, variable electric field, steady, absence of pressure, and suction/injection effect defined above:

$$F \frac{du}{d\xi} = \left(1 + \frac{1}{\beta}\right) \frac{1}{\xi} \frac{d}{d\xi} \left[\mu(T) \xi \frac{du}{d\xi} \right] + g \rho_0 \cos \alpha [k_a(T - T_0) + k_b(T - T_0)^2] - \left[\frac{\sigma^* B_0^2}{\rho_0} + \frac{\mu(T)}{k_p} \left(1 + \frac{1}{\beta}\right) \right] u, \quad (6)$$

$$F \frac{dW}{d\xi} = + \left(1 + \frac{1}{C}\right) \frac{\mu(W)}{\rho_0 c_p} \left(\frac{du}{d\xi}\right)^2 + \frac{Q^*}{\rho_0 c_p} (W - W_0) + \frac{1}{\rho_0 c_p} \frac{1}{\xi} \frac{d}{d\xi} \left[\kappa(W) \xi \frac{dW}{d\xi} \right] \quad (7)$$

Subject to the boundary conditions

$$u = \left(1 + \frac{1}{C}\right) \beta_v \lambda \frac{du}{d\xi}, W = W_1 + \beta_t \frac{2\gamma}{\gamma + 1} \frac{\lambda}{Pr} \frac{dW}{d\xi} \text{ at } 0 \quad (8)$$

$$u = - \left(1 + \frac{1}{C}\right) \beta_v \lambda \frac{du}{d\xi}, W = W_0 - \beta_t \frac{2\gamma}{\gamma + 1} \frac{\lambda}{Pr} \frac{dW}{d\xi} \text{ at } 1$$

where

$$\xi = \frac{t - d_0}{h}, h = C - C_0, f = \frac{u}{h_0}, \eta = \frac{C_0}{C_1}, h_0 = \frac{\rho_0 g k_a (W_1 - W_0)}{\mu_0^2} h^2, \theta = \frac{W - W_0}{W_1 - W_0}, \beta_v = \frac{2 - \sigma_v}{\sigma_v}, \beta_t = \frac{2 - \sigma_t}{\sigma_t}, \lambda = \frac{\sqrt{\pi R T_0 / 2 \mu_0}}{\rho_0} \quad (9)$$

equation (6) and (7) becomes

$$\frac{d\theta}{dW} \frac{\delta Pr}{\eta + (1 - \eta) w Pr} \left\{ \chi \theta + Ec e^{-B_1 \theta} \left(1 + \frac{1}{C}\right) \left(\frac{df}{dw}\right)^2 \right\} \frac{1}{\eta + (1 - \eta) t \frac{d}{dw} \left[[\eta + (1 - \eta) W] e^{-B_2 \theta} \frac{d\theta}{dw} \right]} \quad (10)$$

$$\frac{d\theta}{dw} \frac{\delta Pr}{\eta + (1 - \eta) w Pr} \left\{ \chi \theta + Ec e^{-B_1 \theta} \left(1 + \frac{1}{\beta}\right) \left(\frac{df}{dw}\right)^2 \right\} \frac{1}{\eta + (1 - \eta) t \frac{d}{dw} \left[[\eta + (1 - \eta) w] e^{-B_2 \theta} \frac{d\theta}{dw} \right]} \quad (11)$$

while boundary conditions become.

$$f = \left(1 + \frac{1}{C}\right) \beta_v Kn \frac{df}{dt}, \theta = 1 + G \beta_v Kn \frac{d\theta}{dt}, \text{ at } w = 0, \quad (12)$$

$$f = - \left(1 + \frac{1}{C}\right) \beta_v Kn \frac{df}{dt}, \theta(t) = -G \beta_v Kn \frac{d\theta}{dt}, \text{ at } w = 1.$$

where

$$\left. \begin{aligned} Ha^2 &= \frac{\sigma_0 B_0^2 (1 - \eta)^2}{\mu_0 \rho}, \varepsilon = (W_1 - W_0) \frac{k_b}{k_a}, \delta = \frac{k_0 (1 - \eta)}{\mu_0}, G = \frac{\beta_t}{\beta_v}, \eta = \frac{d_0}{d_1}, Kn = \frac{\lambda}{h}, Pr = \frac{c_p \mu_0}{k_0}, Da = \frac{k_p}{(1 - \eta)^2}, \\ Ec &= \frac{h^0}{\rho c_p (W_1 - W_2)}, \beta_t = \frac{2 - \sigma_t}{\sigma_t} \frac{\gamma}{\gamma + 1} \frac{1}{Pr}, B_3 = \gamma_0 (W_1 - W_0), B_1 = \gamma_1 (W_1 - W_0), B_2 = \gamma_2 (W_1 - W_0), \chi = \frac{Q^*}{\mu_0 c_p} \eta^2 \end{aligned} \right\} \quad (13)$$

We present the flow volumetric rate as follows;

$$Q(w) = 2\pi \int_0^1 t f(w) dw \quad (14)$$

The Skin friction and Nusselt number accordingly.

$$\tau_{0,1} = \left(1 + \frac{1}{C}\right) \frac{df}{dw} \Big|_{w=0,1}, Nu_{0,1} = - \frac{d\theta}{dw} \Big|_{w=0,1}. \quad (15)$$

2.1. Spectral collocation method (SCM)

SCM is an approximate solution method for the differential equation of the form:

$$L(u(z)) + g = 0$$

with boundary conditions (BCs) in the domain D . L denotes differential operator on dependent function $u(z)$, and g is a known function. A solution satisfying boundary conditions (BCs) is assumed for $u(z)$ as

$$u = \sum_{i=0}^N d_i T_i(2z - 1) \quad (16)$$

Here, d_i are the unknown coefficients of trial functions $T_i(2z - 1)$ to be determined. $T_i(2z - 1)$ are shifted Chebyshev base function from $[-1,1]$ to $[0,1]$. Equation (11) and (12) is substituted into equation (17), resulting in error or residue. This error is forced to vanish by using the collocation method as follows

$$\text{for } \delta(z - z_j) = \begin{cases} 1, & z = z_j \\ 0, & \text{otherwise,} \end{cases} \tag{17}$$

$$\int_0^1 R_u(z, d_i) \delta(z - z_j) dz = R_u(z_j, d_i) = 0, \quad \text{for } j = 1, \quad 2, \dots, N - 1 \tag{18}$$

where $z_j = \frac{1}{2} \left(1 - \cos \left(\frac{j\pi}{N} \right) \right)$ are shifted Gauss-Lobatto points. As such, Equation (19) forms a system of algebraic equations to be solved to obtain the values of constant coefficients d_i

2.2. Application of spectral collocation method (SCM)

Solutions are assumed for $f(\eta)$, $\theta(\eta)$, $\phi(0)$ respectively as follows:

$$f(t) = \sum_{i=0}^N a_i T_i(2\eta - 1), \quad \theta(\eta) = \sum_{i=0}^N b_i T_i(2\eta - 1) \tag{19}$$

a_i and b_i are unknown coefficients to be determined, and $T_i(2\eta - 1)$ are the shifted Chebyshev base function. To obtain constant coefficients values, equation (19) is substituted into boundary conditions to have

$$\begin{aligned} \left[\sum_{i=0}^N a_i T_i(2\eta - 1) - \left(1 + \frac{1}{\beta} \right) \beta_v Kn \frac{d}{dt} \sum_{i=0}^N a_i T_i(2\eta - 1) \right]_{t=0} &= 0, \\ \left[\sum_{i=0}^N a_i T_i(2\eta - 1) - 1 - G \beta_v Kn \frac{d}{dt} \sum_{i=0}^N a_i T_i(2\eta - 1) \right]_{t=0} &= 0, \\ \left[\sum_{i=0}^N a_i T_i(2\eta - 1) + \left(1 + \frac{1}{\beta} \right) \beta_v Kn \frac{d}{dt} \sum_{i=0}^N a_i T_i(2\eta - 1) \right]_{t=1} &= 0, \\ \left[\sum_{i=0}^N a_i T_i(2\eta - 1) + G \beta_v Kn \frac{d}{dt} \sum_{i=0}^N a_i T_i(2\eta - 1) \right]_{t=1} &= \end{aligned} \tag{19}$$

In the same manner, equation (20) is also substituted into Equation (11) and (12) to yield residues $R_u(\eta, a_i)$ and $R_\theta(\eta, a_i, b_i)$. As such, the residues are minimized using collocation method as follows

$$\int_0^1 R_f \delta(\eta - \eta_j) d\eta = R_f(\eta_j, a_i) = 0, \quad \text{for } j = 1, \quad 2, \dots, N - 1 \tag{20}$$

$$\int_0^1 R_\theta \delta(\eta - \eta_j) dy = R_\theta(\eta_j, a_i, b_i) = 0, \quad \text{for } j = 1, \quad 2, \dots, N - 3 \tag{21}$$

Table 1. SCM solutions in various approximation orders of convergence when $Ha = 1, \eta = 0.5, \beta = 0.2, Da = 1, \varepsilon = 1.5, B_1 = B_2 = B_3 = 0.2, Pr = 0.71, S = \pm 0.5, \alpha = \frac{\pi}{3}, \chi = 0.1, G = 5, \beta_v kn = 0.05$, where $\eta_j = \frac{1}{2} \left(1 - \cos \left(\frac{j\pi}{N} \right) \right)$. Thus, Eqs. (15-17) produce $2N+2$ system of algebraic equations with $2N+2$ unknown coefficients (a_i, b_i) . The equations are solved by the Newton method using the Mathematical symbolic package MATHEMATICA 11.3 to obtain the values of constant coefficients.

Table 2. SCM solutions in various approximation orders of convergence

Number of iteration (N)	$-f''(\eta)$	$-\theta'(0)$	$\varphi'(0)$
4	3.054620	0.233124	0.358571
6	3.004633	0.180744	0.297306
8	3.002122	0.98752	0.06982
10	3.001933	0.987525	0.06982
12	3.001933	0.98752	0.06982
14	3.001933	0.180557	0.296766
16	3.001933	0.180557	0.296766
20	3.001933	0.180557	0.296766
24	3.001933	0.180557	0.296766
30	3.001933	0.180557	0.296766

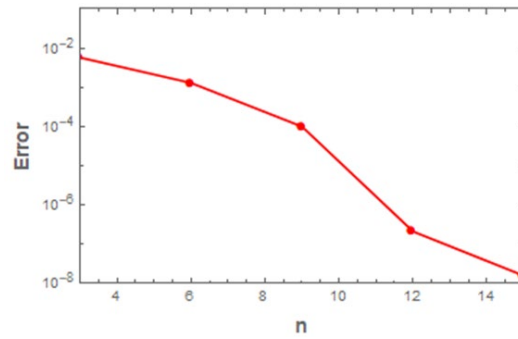


Figure. 2. Minimized residual error

3. Validation, computational results, and discussion

In the context of the mentioned structure, the thermophysical properties of Casson flow on the nonlinear convective flow of blood rheological motion in annular micro-channel with porosity using numerical. The values $Ha = 1, \eta = 0.5, \beta = 0.2, Da = 1, \varepsilon = 1.5, B_1 = B_2 = B_3 = 0.2, Pr = 0.71, S = \pm 0.5, \alpha = \frac{\pi}{3}, \chi = 0.1, G = 5, \beta_{vkn} = 0.05$, as the default flow parameters for this numerical simulation, unless otherwise noted, have particularly been chosen for all table and graphical illustrations. To further confirm the results, a relation between the Spectral collocation method (SCM) and homotopy analysis method (HAM) is shown in Table 2, also the difference between the Spectral collocation method (SCM) and homotopy analysis method (HAM) is denoted by d . From Table 2, It has been found that B_2 variable thermal conductivity, β Casson parameter, and Ha Hartman number Parameters have a propensity to enhance Skin friction, while B_2 variable thermal conductivity, B_1 variable viscosity, and α inclination angle tend to slow it down. The heat transfer is enhanced when B_1 variable viscosity α and c Casson parameter are increased. An increase in B_2 variable thermal conductivity, B_3 variable electrical conductivity, and Ha parameter indicates a reversal of the trend. Figure 2(a,b) presented in numerical form in Table 4 Table 5. Table 4 shows that B_3 variable electrical conductivity has a minor effect on fluid temperature, but this effect is not visible on the graph. Table 4 shows that temperature continues to fall from $\eta=0.1$ to $\eta=0.4$, while from $\eta=0.6$ to $\eta=1.0$, B_2 variable thermal conductivity shows an ability to reduce the fluid temperature.

Table 3. Comparison of the Spectral collocation method (SCM) and homotopy analysis method (HAM) with difference values

c	B_1	K_a	B_2	B_3	SCM	HAM	$ d $
0.4					5.21464	5.21165	0.00000
0.5					5.24191	5.24191	0.00000
	0.3				5.19715	5.19815	0.00000
		0.5			5.25149	5.25149	0.00000
		0.04			5.10386	5.10383	0.00003
		0.06			5.10672	5.10668	0.00004
				0.9	5.21544	5.15543	0.00001
				1.8	4.09825	4.09826	0.00001
			0.2		5.24885	5.24884	0.00001
			0.5		5.19233	5.19432	0.00001

Table 3. Values of skin-friction, and Nusselt number for different parameters

B_1	B_2	B_3	α	β	Ha	Skin friction	Nusselt number
0.7						5.68857	2.39230
1.5						5.63610	2.41282
2.0						5.60342	2.49307
	0.01					5.59999	1.49146
	0.05					5.60166	1.47690
	0.07					5.60333	1.46252
		0.1				5.66937	1.49957
		0.2				5.52734	1.49013
		0.4				5.49573	1.48277
			$\pi/6$			1.66837	1.50513
			$\pi/5$			5.65878	1.40524
			$\pi/4$			5.64368	1.50530
				0.3		5.58279	1.50255
				0.5		5.63016	1.51270
				0.9		5.67990	1.52368
					0.4	5.60923	1.47887
					0.6	5.64416	1.39079
					0.8	5.69392	1.29054

Table 4. Effect of variable electrical conductivity (B_3) on the temperature profile

η	0.1	0.2	0.4	0.6	0.8	1.0
$B_3=0.1$	1,099500	0.518484	0.247139	0.119627	0.058668	0.029054
$B_3=0.3$	1,099500	0.509459	0.243169	0.119894	0.060664	0.031242
$B_3=0.5$	1,099500	0.502553	0.240365	0.120271	0.062239	0.032888
$B_3=0.7$	0,006846	0.003030	0.001044	$-8.361909 \times 10^{-18}$		
$B_3=0.9$	0,008017	0.003691	0.001318	$-1.928525 \times 10^{-17}$		
$B_3=1.0$	0,008867	0.004169	0.001514	$-1.324082 \times 10^{-17}$		

Table 5. Effect of variable electrical conductivity (B_3) on the temperature profile

η	0.1	0.2	0.4	0.6	0.8	1.0
$B_3=0.1$	1.110223×10^{-16}	1.034678	0.794341	0.670473	0.599357	0.565011
$B_3=0.3$	1.110223×10^{-16}	1.094751	0.855088	0.716909	0.631038	0.585281
$B_3=0.5$	2.220446×10^{-16}	1.141179	0.900692	0.751129	0.654171	0.600058
$B_3=0.7$	0.547432	0.534347	0.529838	0.527093	0.524875	
$B_3=0.9$	0.559761	0.541413	0.533488	0.528522	0.524875	
$B_3=1.0$	0.568785	0.546624	0.536206	0.529597	0.524875	

Figure 2(a, b). Shows the thermal properties for different values for the rarefaction parameter, for velocity and temperature. A rise in the rarefaction value suggests an increase in speed and temperature, which reduces the inhibiting impacts of the boundaries. The fluid velocity is much higher near both boundaries. This is because, due to the rise in $BvKn$, speed and temperature jumps are increased, which reduces the amount of heat transfer to the fluid from the cylinder surfaces. The decrease in the thermal transfer lowers fluid efficiency and reduces fluid speed far from the outside surface of the internal cylinder (near the interior surface of the exterior cylinder). The increase in speed caused by declining frictional retardants close to the surfaces of the cylinders neutralizes velocity reduction because of the decrease in heat transfer. Furthermore, as the radius ratio (η) increases, the slip due to rarefaction increases. The effect of the curvature radius on flow and thermal profiles in Figure 2(c) is graphically illustrated. The free fluid flow area physically permits fluid particles to flow freely, resulting in higher speed and power owing to collisions between the medium and the liquid particles, which reduce the inner binding force inside the fluid particles. A significant annular

gap ratio with both constant and variable thermal effects is shown in Figure 2(d). It's worth noting that a higher temperature on both surfaces is correlated with a higher ratio of curvature. Similarly, an increase in Darcy numbers and continual infusion of Casson fluid promotes the velocity area. (Fig. 2(e and f)). Figure 2e As the number of Darcy rises, so does the permeability of the fluid. The fluid's speed rises with the continual rising, as seen in Figure. 2f. The neutralization of a non-Newtonian fluid to a Newtonian fluid is physically achieved. Figure 2 depicts the amount of results obtained as a result of the initial layer improvement and the corresponding outcomes (e, f).

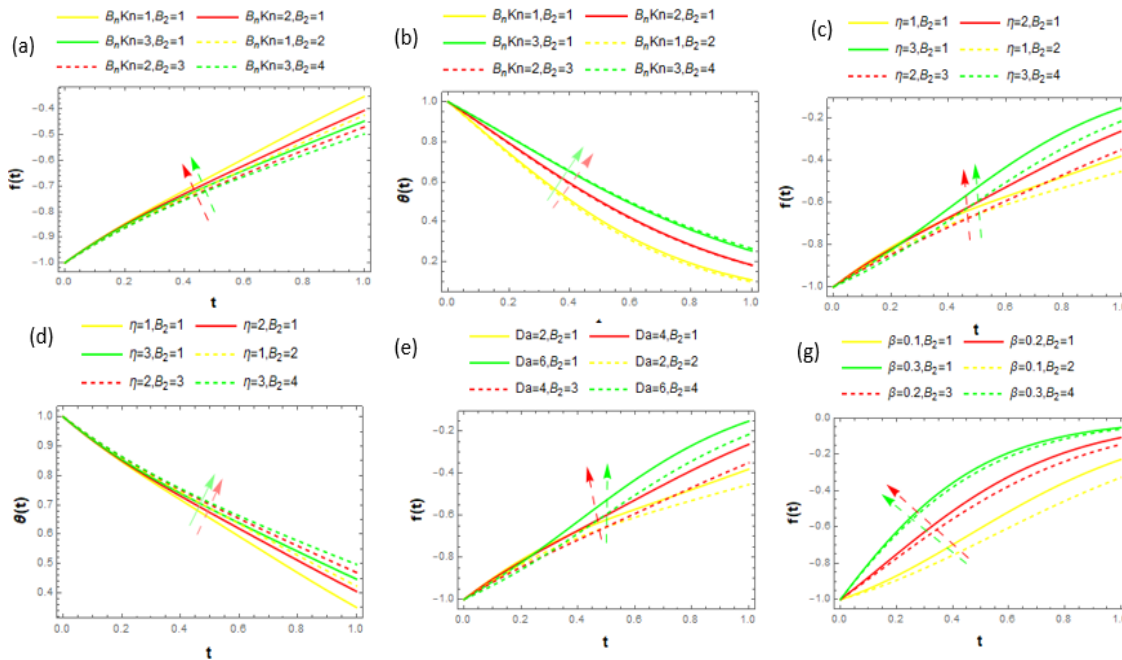


Figure 1(a, b, c, d, e, f). thermo properties, rarefaction parameter, radius ratio, Darcy, Casson parameter

Figure 3(a, b). Depicts the effect of thermophysical on flow velocity and temperature under the impact of suction/injection. The suction force on the flow particles, caused by a low pressure, dominates the velocity field in the case of injection in flow ranges (insertion of fluid particles). The suction effect mechanically transports fluid particles near to the cylinder surfaces, whereas the injection effect indicates a continual buildup of fluid particles. Variable viscosity has a favorable influence on the flow field, but this is due to flow resistance, whereas thermal conductivity reduces both speed and thermal profiles. Both the speed and thermal profiles were lowered as a result of the thermal conductivity Figure 3 (b, c)). The influence of the Hartmann number on velocity is shown in Figure 3 (d, e) and the variable electrical field effect. As the number of Hartmann increases, fluid velocity, and temperature decrease. It reduces the velocity of the fluid and the effects of variable characteristics are determining the flow speed in the area. However, the field in the area decreased. The flow field has negatively affected the performance of the electric variable field (see Figure 3 (f)) This is true physically since, in the existence of electrically conducting liquids, the impact of the magnetic field generates the Lorentz force which leads to fluid flow retardation and a reduction of the speed of flow through the flow. The effect of the non-linear convection parameter and angle of inclination on the flow rate is shown in (see Figure 3 (g)). The increase in the non-linear convection term increases the speed of the flow. Variable thermal effects are greater than constant thermal effects in both cases of the speed(see Figure 3 (h)). The flow rate is reduced by an increased inclination angle. The thermal of a heat generation parameter is shown in (see Figure 3 (i)). The effect of constant thermal, variable thermal and heat generation on temperature of the liquid increase.

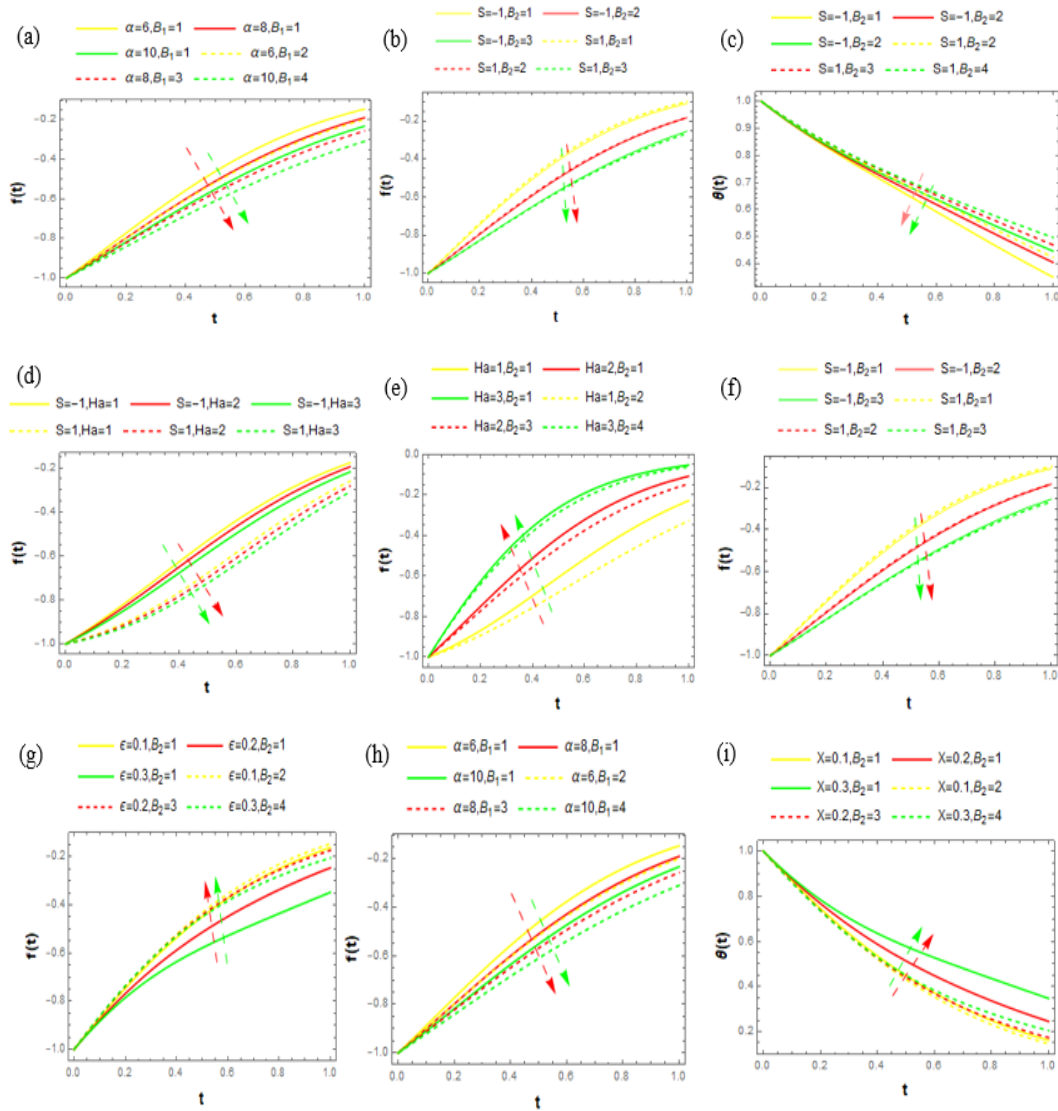


Figure 2(a, b, c, d, e, f, g, i). Effect of variable properties under Suction/Injection condition, Suction/Injection and Hartmann number, variable properties, variable electrical field (f)

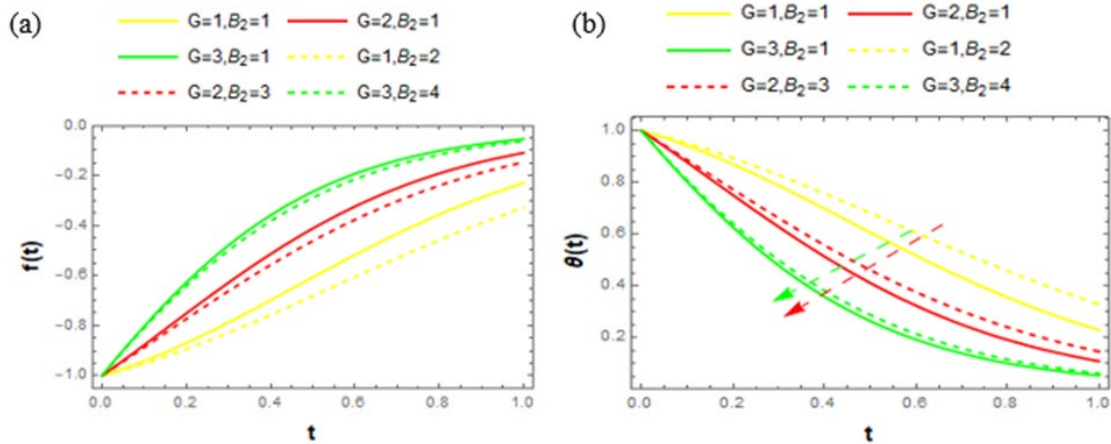


Figure 3(a, b). impact of thermo properties on velocity and temperature for different values of the fluid-wall interaction parameter

Figure 4(a,b) shows the effect on velocity and temperature profile of the the fluid wall interaction parameter. a significant decrease in fluid velocity and template, leading to a slip velocity increase close to the outside surface of the inner cylinders while the reverse performance on the inner surface is detected.

4. Conclusion

To examine the performance of Casson velocity fluid, temperature field, the variable conductivity, viscosity, and variable electrical field (VEF) was used. the best possible solution for the skin friction and heat transfer rate of blood rheological (Casson) through an Inclined Annular Micro-Channel using Spectral collocation method (SCM)).

1. It was deduced that; the flow field was reduced as variable thermal and electrical field parameters were increased., while the viscosity parameter resulted in a trend of appreciation.
2. The curvature radius of both the momentum and energy distributions was increased.,
3. As compared to the insertion of fluid particles, a higher Darcy number leads to a higher flow rate, and,
4. The flow fields are control by force exerted on the liquid particles by partial vacuum.

For future investigation: The dynamics in which the fluid behavior is evaluated and regulated through a microchannel in the microfluidics are a reduction mechanism in the development of devices and are an enhancing factor in thermal energy. This device can be used on a micro heat exchanger, store cooling of grain, geothermal systems, oil extraction, groundwater contamination, nuclear waste storage, MHD micropumps, multidisciplinary thermal insulation areas, etc. To this purpose, investigations of a blood rheological (Casson) nonlinear convection flow mechanism in a ring microchannel containing a porous medium become crucial, as they enable the industry to understand and enhance the efficiency of the flow process. More studies may also include research into various fluid rheology and study of fluid thermophysical properties to predict proper flow (to achieve a remarkable convection process). Therefore SCM, implementation can be expanded to include different and multi-dimensional flow problems.

Acknowledgment

The author appreciates the excellent research facilities provided by Kwara State University.

Conflict of interest

No declarations by the writer.

Nomenclature

B_0	magnetic flux density	η	radii ratio parameter
C_p	specific heat at constant pressure	Da	Darcy Parameter
$\beta t, \beta v$	dimensionless parameter	k_0	constant suction/injection velocity
γ	ratio of specific heat	g	gravitational acceleration
d_0	radius of inner porous cylinder	R	specific gas constant
d_1	radius of the outer porous cylinder	K_a	thermal conductivity
β	Casson parameter	ρ	fluid density
χ	heat source parameter	B_1	variable viscosity
λ	molecular mean free path	B_2	variable thermal conductivity
T_0	temperature at the inlet	B_3	variable electrical conductivity
T_1	temperature at the outlet	σ_v	thermal accommodation
Kn	Knudsen number	σ_t	tangential momentum accommodation
α	inclination angle	θ	dimensionless temperature
Ha	Hartman number	Ec	Eckert number
ε	non-linear thermal convection	T	fluid temperature
G	wall-fluid interaction parameter	f	dimensionless axial velocity
Q	volume flow rate	u	dimensional axial velocity
μ_0	dynamic viscosity	ξ	dimensional radial coordinates
δ	suction/injection parameter	t	dimensionless radial coordinate
ρ_0	fluid mixture density	h	dimensionless gap between the cylinders
Pr	Prandtl number		

References

- [1] Obalalu AM, Ajala OA, Adeosun AT, Wahaab FA, Oluwaseyi A, and Adebayo LL. Natural Convective Non-Newtonian Casson Fluid Flow in a Porous Medium with Slip and Temperature Jump Boundary Conditions. *Pet Coal*, 2020; 62 (4): 1532-1545.
- [2] Obalalu AM, Wahaab FA, and Adebayo LL. Heat transfer in an unsteady vertical porous channel with injection/suction in the presence of heat generation. *Journal of Taibah University for Science*, 2020; 14 (1): 541-548.
- [3] Obalalu AM, Kazeem I, Abdulrazaq A, Ajala OA, Oluwaseyi A, Adeosun AT, Adebayo LL, and Wahaab FA. Numerical simulation of entropy generation for casson fluid flow through permeable walls and convective heating with thermal radiation effect. *Journal of the Serbian Society for Computational Mechanics*, 2020; 14 (2): 503-519.
- [4] Hartmann J, and Lazarus F. Hg-dynamics II. Theory of laminar flow of electrically conductive Liquids in a Homogeneous Magnetic Field, 1937; 15 (7):
- [5] Jha BK, and Malgwi PB. Hall and ion-slip effects on MHD mixed convection flow in a vertical microchannel with asymmetric wall heating. *Engineering Reports*, 2020; 2 (9): e12241.
- [6] Roja A, and Gireesha B. Hall effects on MHD couple stress fluid flow through a vertical microchannel subjected to heat generation: A numerical study. *Heat Transfer*, 2020; 49 (8): 4738-4758.
- [7] Khan ZH, Gul R, and Khan WA. Effect of variable thermal conductivity on heat transfer from a hollow sphere with heat generation using homotopy perturbation method. *Heat Transfer in Energy Systems. Heat Transfer in Nanostructure and Nanoporous Materials*, Journal Type of Article 48470, 301-309. <https://doi.org/10.1115/HT2008-56448>
- [8] Kafoussias N, and Williams E. The effect of temperature-dependent viscosity on free-forced convective laminar boundary layer flow past a vertical isothermal flat plate. *J Acta Mechanica*, 1995; 110 (1): 123-137.
- [9] Myers T, Charpin J, and Tshehla M. The flow of a variable viscosity fluid between parallel plates with shear heating. *Applied Mathematical Modelling*, 2006; 30 (9): 799-815
- [10] Rahman M, Uddin M, Bég OA, and Kadir A. Influence of variable viscosity and thermal conductivity, hydrodynamic, and thermal slips on magnetohydrodynamic micropolar flow: a numerical study. *Heat Transfer—Asian Research*, 2019; 48 (8): 3928-3944.
- [11] Singh AK, Singh A, and Roy S. Analysis of mixed convection in water boundary layer flows over a moving vertical plate with variable viscosity and Prandtl number. *International Journal of Numerical Methods for Heat Fluid Flow*, 2019; 29(2): 602-616.
- [12] Qasim M, Riaz N, Lu D, and Afridi M. Flow over a Needle Moving in a Stream of Dissipative Fluid Having Variable Viscosity and Thermal Conductivity. *J Arabian Journal for Science Engineering*, 2021: 1-8.
- [13] Adeniyani A, Mabood F, and Okoya S. Effect of heat radiating and generating second-grade mixed convection flow over a vertical slender cylinder with variable physical properties. *International Communications in Heat Mass Transfer*, 2021; 121: 105110.
- [14] Jenifer AS, Saikrishnan P, and Lewis RW. Unsteady MHD Mixed Convection Flow of Water over a Sphere with Mass Transfer. *Journal of Applied Computational Mechanics*, 2021; 7 (2): 935-943.
- [15] Kataria HR, and Patel HR. Radiation and chemical reaction effects on MHD Casson fluid flow past an oscillating vertical plate embedded in porous medium. *Alexandria Engineering Journal*, 2016; 55(1): 583-595.
- [16] Makinde OD, and Sankar M. Numerical investigation of developing natural convection in vertical double-passage porous annuli. *Numerical Investigation of Developing Natural Convection in Vertical Double-Passage Porous Annuli. Defect and Diffusion Forum*, 2018; 387: 442-460.
- [17] Sankar M, Girish N, and Siri Z. Fully developed magnetoconvective heat transfer in vertical double-passage porous annuli. in *Flow and transport in subsurface environment*: Springer, 2018, pp. 217-249.
- [19] Obalalu AM, Wahaab FA, and Adebayo LL. Heat transfer in an unsteady vertical porous channel with injection/suction in the presence of heat generation. *Journal of Taibah University for Science*, 2020; 14(1): 541-548.
- [20] Ajala O, Adegbite P, Abimbade SF, Obalalu AM. Thermal radiation and convective heating on hydromagnetic Boundary layer flow of nanofluid past a permeable stretching Surface. *International Journal of Applied Mathematics & Statistical Sciences*, 2019; 2(8): 43-58.
- [21] Casson N. A flow equation for pigment-oil suspensions of the printing ink type. *Rheology of disperse systems*, 1959
- [21] Casson N. A flow equation for pigment-oil suspensions of the printing ink type. In: Mill CC, Ed., *Rheology of Disperse Systems*, Pergamon Press, Oxford, 84-104.

- [22] Mukhopadhyay S, Vajravelu K, and van Gorder RA. Casson fluid flow and heat transfer at an exponentially stretching permeable surface. *Journal of Applied Mechanics*, 2013; 80 (5).
- [23] Shrama P, and Singh G. Steady MHD natural convection flow with variable electrical conductivity and heat generation along an isothermal vertical plate. *J Journal of Applied Science Engineering*, 2010; 13 (3): 235-242.
- [24] Chen Y, and Or D. Effects of Maxwell-Wagner polarization on soil complex dielectric permittivity under variable temperature and electrical conductivity. *WRR*, 2006; 42 (6).

To whom correspondence should be addressed: Dr. Adebowale Martins Obalalu, Department of Statistics and Mathematical Sciences, Kwara State University, Malete, Nigeria, E-mail: adebowale.obalalu17@gmail.com